Acta Polytechnica **63**(4):268–272, 2023
https://doi.org/10.14311/AP.2023.63.0268
© 2023 The Author(s). Licensed under a CC-BY 4.0 licence
Published by the Czech Technical University in Prague

SHOCK WAVE CONFIGURATION IN A TRANSONIC FLOW THROUGH A MID-SECTION OF A LAST STAGE TURBINE BLADE CASCADE EQUIPPED WITH A PART-SPAN CONNECTOR

Tomáš Radnic[a,*], Pavel Šafařík[a,b], Martin Luxa[b], David Šimurda[b]

[a] *Czech Technical University in Prague, Faculty of Mechanical Engineering, Department of Fluid Dynamics and Thermodynamics, Technická 1902/4, 162 00 Prague, Czech Republic*

[b] *Czech Academy of Sciences, Institute of Thermomechanics, Dolejškova 1402/5, 182 00 Prague, Czech Republic*

[*] corresponding author: radnic@it.cas.cz

Abstract. This paper deals with the study of a flow field and namely the configuration of shock waves in a blade cascade equipped with a part-span connector called tie-boss. The cascade consists of prismatic blades formed from the mid-section of a very long last-stage blade of a steam turbine. The study is based on numerical simulations of the flow through a cascade that was previously tested in a wind tunnel. Commercial software Ansys CFX was used for the simulations and Ansys ICEM for the mesh generation. The computational domain contains non-homogenous mesh interfaces. The simulations showed that the presence of the tie-boss has a profound effect on the configuration of the shock waves. The blade exit shock waves are disturbed and new lateral shock waves are introduced into the flow.

Keywords: Transonic flow, blade cascade, part-span connector, numerical simulation, shock wave, steam turbine.

1. Introduction

A modern steam turbine contains very long last-stage rotor blades. The elongation of the blades had improved efficiency by increasing the area of the exit annulus and possibly the higher mass flow achieved in a such equipped low-pressure cylinder. The downside of this approach is the utilisation of long thin blades which are very prone to deformation and flutter. Therefore, a solution was required that would shift the natural frequency of the blades above its operating frequency.

In the past this role was fulfilled by stabilising wires, which were mounted through holes drilled in the blades. The modern solution relies on connectors that come into contact with untwisting of the blade. As the modern last-stage blade has a wide variety of inlet speeds, it has a variating, non-prismatic, shape. This shape causes the blade to untwist as the rotor speeds up. Very long last-stage blades are usually equipped with a tip connector and a part-span connector.

This paper focuses on the part-span connector, called the tie-boss, and its influence on a model flow field in model research. Because the tie-boss is mounted in a cut which is 610 mm above the root of the blade, the flow field is transonic. Therefore, the tie-boss is expected to have a profound effect on the configuration of shock waves.

2. State of the art

Investigations of the part-span connector under subsonic flow conditions have been carried out by Bruggemann et al. [1], Bin Li et al. [2] and by Häfele et al. [3, 4]. These works by various research teams around the world showed that part-span connectors induce vorticial structures, cross flow, and increased losses. However, as the investigated cases have been subsonic, no shock waves were present.

The investigation by Liu et al. [5] was focused on the conditions on a blade stage in off-design conditions in a transonic flow regime. However, the investigation was concerned with the performance of the blade and with the conditions between the individual blades rather than with the details of the flow past the part-span connector, hence no shock wave configuration was investigated. Nevertheless, the investigation showed that there is a considerable loss of total pressure and inlet and outlet swirl angle in the area of the part-span connector. A flow deflection in a supersonic flow field will certainly result in a shift in the shock wave configuration.

An experimental research on identical cascades was performed by Radnic et al. [6]. The research showed that the tie-boss had radically affected the flow field parameters. Pneumatic measurements showed an increase in kinetic energy loss, exit flow angle, and curvature of the exit shock waves. Surface flow visualisation showed curved impingement traces of the exit shock waves, which at the time led to the conclusion that the shock wave configuration had been significantly altered.

The measured data were re-examined, see Figure 1. In the green area, there are local flow separations caused by the interaction of the inner branch of the exit shock wave with the boundary layer. This shock wave trace is clearly curved and it is debatable whether

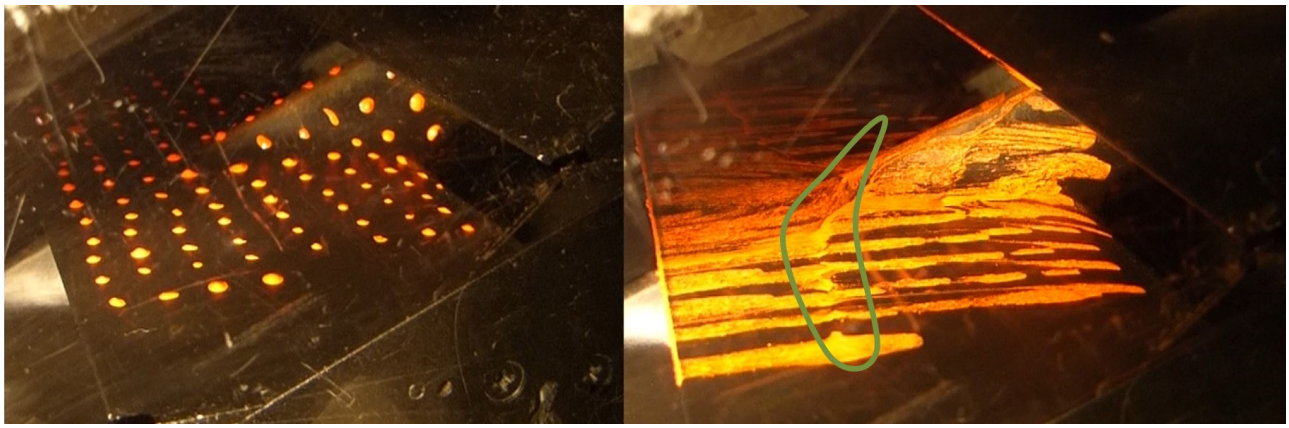

FIGURE 1. Surface flow visualizations prior (left) and during (right) measurement.

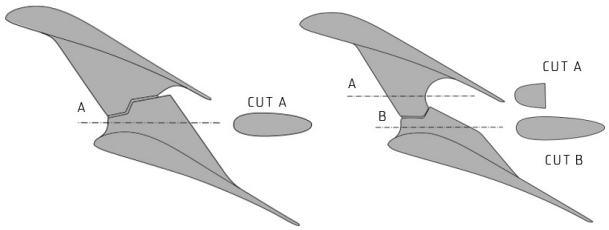

FIGURE 2. Picture of oval tie-boss (left) and tailored tie-boss (right).

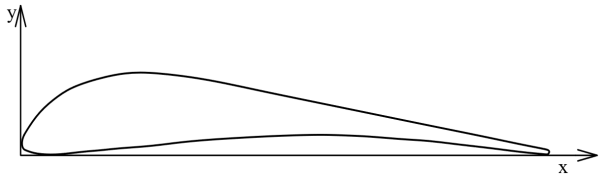

FIGURE 3. Mid-section of 1220 mm long blade.

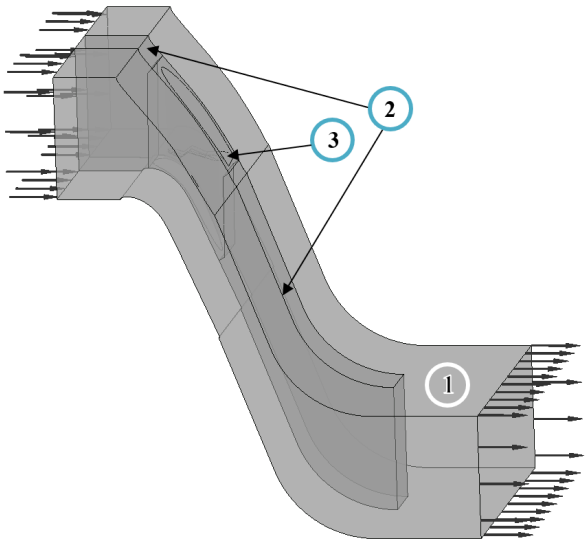

FIGURE 4. Computational domain zoning.

it is present in the area of the tie-boss body. More detailed photographs taken after the tunnel has been shut off cannot be used because the viscous oil is moved around by the waning flow.

Further numerical investigations by Radnic et al. [7] showed a complicated shock wave configuration, including curved and mutually interacting shock waves and vorticial structures in the flow field.

A meticulous numerical study on was therefore required to simulate the shock wave configuration in sufficient detail. Better shock wave visualisation techniques need to be used and the resolution of these methods must capture even the less significant shock waves.

3. Materials and methods

Presented research is a model research on a prismatic blade cascade. The cascade is equipped with two types of the tie-boss, oval and tailored, see Figure 2. The oval type of the tie-boss has straight and oval trailing edge and apart from the notches, a constant cross section. The tailored tie-boss has a cylindrical flat face as a trailing edge of the upper part. The lower part of the tailored tie-boss is longer than the top part and it has a round trailing edge with a flat surface on its top.

The tie-boss is mounted on a prismatic blade formed from the mid-section of a 1220 mm long last-stage blade, see Figure 3.

The cascade had a chord of $c = 80$ mm, pitch $t = 58.34$ mm. The span of the cascade was $l = 160$ mm, identical to the experimental setup. The stagger angle of the cascade was $\gamma = 55.52°$. Only the nominal, $\iota = 0°$, flow regime has been considered for this investigation. The inlet Mach number was $M = 0.3$, the outlet Mach number was $M = 1.44$. The inlet flow angle was $\beta_1 = 30.9°$.

The computational mesh was generated in the Ansys ICEM software. The computational domain was divided into three zones, see Figure 4.

Zone 1 contained the outer mesh, Zone 2 contained the inner parts of the mesh upstream and downstream of the tie-boss region, and Zone 3 was situated around the tie-boss body. Zones 1 and 2 were meshed using blocking, incorporating the stepped periodic tech-

nique, which allowed for a conformal 1:1 periodic mesh interface and avoided the generation of highly skewed cells. Zone 3 has been generated using the octree flooding algorithm with the post inflation boundary layer refinement. The interfaces in-between the zones were non-homogenous. This approach was chosen because the complicated shape of the tie-boss prevented the generation of structured mesh and the flooding algorithm generated a good enough mesh, while in the outer regions, the structured mesh generation provided a high quality mesh with fewer elements than would have been possible with the flooding. The outlet region of the mesh has been greatly coarsened to prevent shock wave reflection on the outlet boundary. The mesh had a total of 6.8 million cells and in the Zone 1, there were 188 cells along the surface of the blade.

The chosen numerical simulation software was Ansys CFX for its good handling of non-homogenous interfaces. The working medium was air, ideal gas. The total energy heat transfer model was utilised with the viscous work consideration. The turbulence viscosity was calculated using the shear stress transport model. The inlet boundary conditions were set to $p_0 = 100\,000\,\mathrm{Pa}$, $T_0 = 298\,\mathrm{K}$, and inlet flow angle corresponding to the nominal inlet angle of the cascade. The periodic boundary condition was set up on top and bottom of the computational domain. The side walls of the domain as well as the blade were set to be no slip walls and the outlet boundary conditions were set to $p_{out} = 30\,000\,\mathrm{Pa}$. No numerical non-reflective conditions were set. The coarsened area at the outlet cancelled out any shock waves that were present but allowed the outlet pressure to be maintained.

The mesh sensitivity analysis showed that a mesh consisting of 6.8 million cells was necessary to provide a sufficient accuracy of the numerical data for the investigation of shock waves. The analysis was performed using various densities of meshes, ranging from 0.8 million to 10 million cells.

The post-processing was done using the Ansys CFX Post. The visualisation of the shock waves was done by creating iso surfaces of a set density gradient. The grey contour colouring of the isosurfaces was done by creating a pitch-wise coordinate. It bears no physical quantity and is used solely to illustrate the shape of the isosurfaces. The density gradient isosurfaces were clipped by an arbitrary value of pressure to eliminate regions upstream of the shock waves, where, in the boundary layer, the selection criterion was met.

The configuration of the shock waves in the interblade channel of the tailored tie-boss is shown in Figure 5. The individual shock waves have been labelled and the labels are identical for laterally symmetrical waves. The shock wave (a) originates at the intersection of the lower part of the tie-boss and the suction side of the blade. There is a change in the curvature of the blade and the tie-boss resulting in a local decrease of shear stress and change of the flow

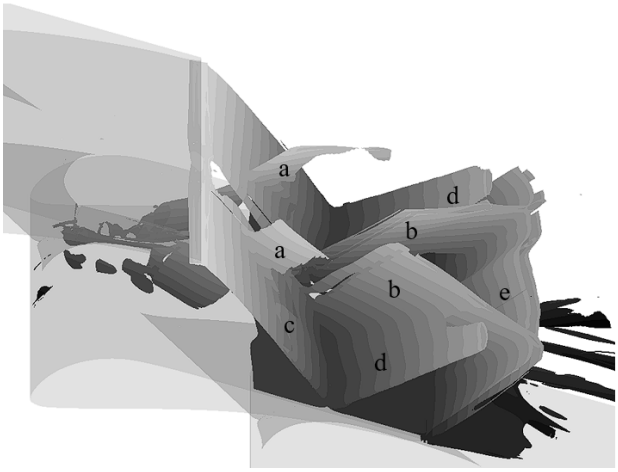

Figure 5. Side view of shock wave configuration for tailored tie-boss.

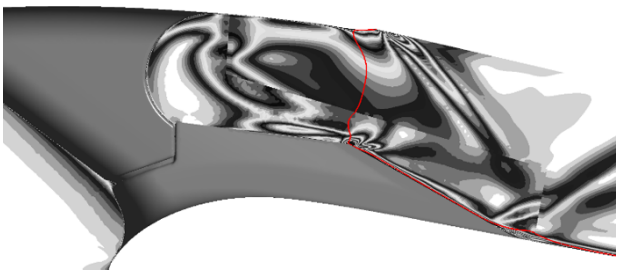

Figure 6. Density gradient and sonic line (red) in the cut in the middle of the channel.

direction.

Presumably, this deflection leads to the creation of the shock wave (a) in a similar manner a shock wave would form around a past flown profile. It should also be noted that this shock wave is relatively weaker than the other shock waves, needing a lower density gradient threshold to show. The shock wave (b) originates near the intersection of the tie-boss trailing edge and the suction side of the blade. It then propagates diagonally, interacting with the shock waves (d) and (e) with which it ultimately seems to merge. At the point of origin of the shock wave (b), there is a small subsonic region, see Figure 6. The shock wave (c) is the inner branch of the upper blade exit shock wave. It is obvious that the shape of the wave is disturbed in the middle, where there is a large wake behind the tie-boss. The visualisation method did not allow the attribution of the phenomena to shock wave, wake or vortex structures, as all of these cause significant density gradients. However, the shear stress distribution on the surface of the blade indicates that there is a continuous interaction in the boundary layer. It would be wrong to assume that the shock waves are interrupted. The shock wave (d) is a regular reflection of the shock wave (c). Near the middle of the channel, the shock wave (d) appears to merge into the shock wave (b). The shape is continuously curved towards the wave (b) and there are no planar shocks inside the pocket formed by it. The shock wave (e) is the outer

branch of the exit shock wave of the bottom blade. It is clear that the shock wave is not planar. In the area of the wake of the tie-boss, there is an upstream curvature. This difference in the shock wave angle is presumably given by the different upstream velocity in the wake of the tie-boss leading to a different shock wave angle. There is another curvature on this shock wave at the point of merger with the diagonally moving shock wave (d). This is also to be expected as the result of the flow deflection induced by the diagonal wave.

Figure 7 depicts the shock wave configuration in the interblade channel of the oval tie-boss. The configuration is very similar to the tailored tie-boss, yet the diagonal shock waves are clearly stronger, and a diamond shaped interaction is formed. The shock wave (a) is consistently stronger than in the case of the tailored tie-boss, originating at a very similar location. Upstream of the point of origin is the same change of curvature and the mechanism of formation of this shock wave is presumed to be identical. The shock wave (b) is also stronger than in the case of the tailored tie-boss and does not merge completely into the shock wave (e). The strength of the shock wave (b) is attributed to the shape of the trailing edge of the oval tie-boss. The trailing edge is much further downstream and does not cause a significant flow separation as compared to the tailored trailing edge. Instead, greater turning of the flow into the wake is present, which must later be accompanied by turning away from the wake and the formation of the shock wave (b). The inner branch of the blade exit shock wave (c) is almost identical to the case of the oval tie-boss. This is to be expected, as except the tie-boss, the interblade channel is identical with an identical mesh. The shock wave (d) bears a strong resemblance to the tailored tie-boss case; however, it is slightly curved by the interaction with the shock wave (a). The shock wave (e) is again the outer branch of the blade exit shock wave. It is clearly deformed by the wake of the tie-boss and by the interaction with shock waves (a) and (b). The curvature of the wave in the wake of the tie-boss is clearly greater than that of the tailored tie-boss. This influence is once again attributed to the position of the trailing edge. Also, the research of the vorticial structures in [7] showed that there are two significant contrarotating vortices behind the trailing edge, which keep the lower momentum fluid in the area of the wake for a longer time.

Figure 8 shows a span-wise distribution of the relative outlet exit angle evaluated by the data reduction method, see [6], in a pitch-wise section across a plane parallel to the plane of the trailing edges. The position of the plane is identical to the traversing plane in [6], which was 22 mm behind the plane of the trailing edges. The data reduction method allows integral parameters of the flow field to be obtained, which then provide a set of representative parameters. In

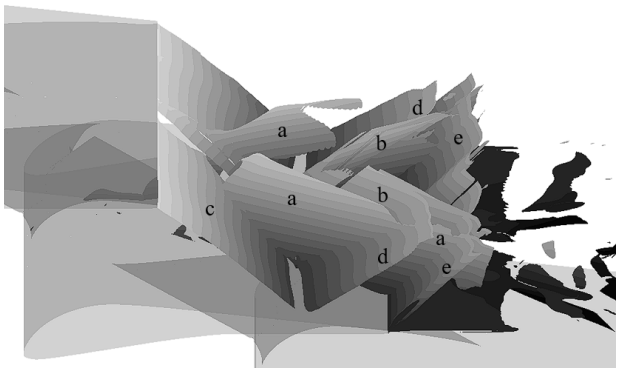

FIGURE 7. Oval tie-boss shock wave configuration.

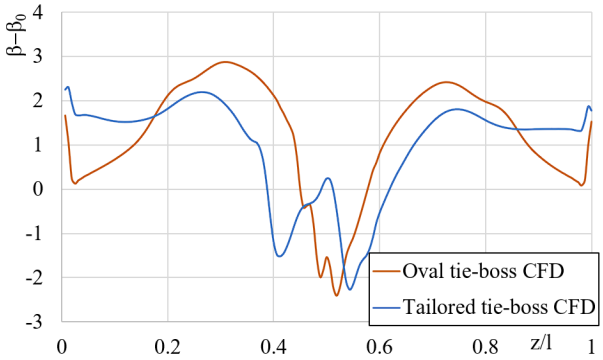

FIGURE 8. Span-wise distribution of the relative outlet exit angle.

this case, the exit flow angle of the cascade has been evaluated. The distribution shows that the oval type tie-boss has caused a greater flow turning and that this turning occurs in the area further away from the tie-boss too. This effect is presumed to be tied to the shock wave configuration, especially the strength of shock waves (a) and (b) in the case of the oval tie-boss, which also shows a greater flow turning in the region outside the direct influence of the tie-boss. The distribution also shows that the relative flow turning in the area of the wake of the tie-boss is of a similar value, yet the width of the affected area is different. This behaviour is believed to be caused by vortices that stay closer to the wake of the tie-boss in the case of the oval one and stray further away in the case of the tailored one.

4. CONCLUSION

The detailed numerical investigation of the interblade channel with the part-span connectors under transonic flow conditions provided critical insight into the configuration of the shock waves. The tie-bosses introduced diagonal shock waves to the flow field and deformed the standard shock waves present in a transonic interblade channel. Both versions of the tie-boss introduced two sets of diagonal shock waves, one originating at the intersection of the tie-boss trailing edge and the blade surface, and the other appearing to originate at the point of change of curvature of the

blade and the tie-boss intersection. The diagonal shock waves are stronger in the case of the oval tie-boss. This finding contradicts the conclusions of [6], where the tie-bosses were assumed to deform only the inner branch of the exit shock wave and it's reflected counterpart. The influence of the tie-boss on the inner and outer branches of the exit shock waves consists of a deformation due to the presence of the wake, thus altering the shock wave angle and passing the said diagonal shock waves, causing a frow turning, which in turn affects the shape of the previously planar shock waves. The connectors have been found to cause significant differences in the exit flow angle. The oval tie-boss causes larger differences in flow turning as well as a larger deformation of the blade exit shock waves. This behaviour is believed to be connected.

A future research is in order to determine the optimised shape or position of the tie-boss in an attempt to minimise the effect of the tie-boss on flow turning and possibly its effects on the blade performance. The part-span connectors shown by other authors often differ in position, size and shape. However, providing a new shape of tie-boss is beyond the scope of this research.

References

[1] C. Brüggemann, M. Schatz, D. Vogt, F. Popig. A numerical investigation of the impact of part-span connectors on the flow field in a linear cascade. In *Proceedings of ASME Turbo Expo 2017: Turbomeachinery Technical Conference and Exposition, Charlotte, NC, USA*, vol. 2A, p. 11. 2017. https://doi.org/10.1115/GT2017-63359

[2] B. Li, J. Li. Numerical investigations on the aerodynamic performance of last stage bucket with part-span connector. In *Proceedings of ASME International Engineering Congress and Exposition 2014, Montreal, Quebec, Canada*, vol. 7, p. 8. 2014. https://doi.org/10.1115/IMECE2014-38039

[3] M. Häfele, J. Starzmann, M. Grübel, et al. Numerical investigations on the impact of part-span connectors on aero-thermodynamics in a low pressure industrial steam turbine. In *Proceedings of ASME Turbo Expo 2014: Turbine Technical Conference and Exposition, Düsseldorf, Germany*, vol. 1B, p. 14. 2014. https://doi.org/10.1115/GT2014-25177

[4] M. Häfele, C. Traxinger, M. Grübel, et al. Numerical and experimental study on aerodynamic optimization of part-span connectors in the last stage of a low-pressure industial steam tubine. *Sage Journals* **229**(5):465–476, 2015. https://doi.org/10.1177/0957650915591906

[5] Y. Liu, Q. Jia, X. Zhou, et al. Experimental study on the aerodynamic characteristics of blades at the last stage of a steam turbine at off-design conditions. *International Journal of Aerospace Engineering* **2022**:8785963, 2022. https://doi.org/10.1155/2022/8785963

[6] T. Radnic, J. Hála, M. Luxa, et al. Aerodynamic effects of tie-boss in extremely long turbine blades. *Journal of Engineering for Gas Turbines and Power* **140**(11):112604, 2018. https://doi.org/10.1115/1.4040093

[7] T. Radnic, J. Hála, M. Luxa, D. Šimurda. Numerical investigations of 3-D flow phenomena in interblade channel with tie-boss. In *Proceedings of 14th Eruopean Conference on Turbomachinery Fluid dynamics & Thermodynamics*, pp. ETC2021–627. 2021. https://doi.org/10.29008/ETC2021-627